Received: 19 May 2025 | Revised: 10 March 2026 | Accepted: 10 March 2026

DOI: 10.1111/joa.70143

Journal of Anatomy | ANATOMICAL SOCIETY WILEY

ORIGINAL ARTICLE

Scaling relationships between Haversian canal-to-secondary osteon and midshaft femur cortical-to-total area in a human autopsy sample

Justyna J. Miszkiewicz[1,2,3] | Laura A. B. Wilson[3,4,5] | Karen M. Cooke[1] | Rita Hardiman[6]

[1]School of Social Science, University of Queensland, St Lucia, Queensland, Australia

[2]Earth, Life, Time Group, Naturalis Biodiversity Center, Leiden, The Netherlands

[3]School of Archaeology and Anthropology, Australian National University, Canberra, Australian Capital Territory, Australia

[4]School of Biological, Earth and Environmental Sciences, UNSW Sydney, Sydney, New South Wales, Australia

[5]ARC Training Centre for Multiscale 3D Imaging, Modelling and Manufacturing, Research School of Physics, The Australian National University, Canberra, Australian Capital Territory, Australia

[6]Melbourne Dental School, University of Melbourne, Melbourne, Victoria, Australia

Correspondence
Justyna J. Miszkiewicz, School of Social Science, University of Queensland, St Lucia, Qld, Australia.
Email: j.miszkiewicz@uq.edu.au

Funding information
Australian Research Council, Grant/Award Number: DE190100068, FT200100822 and FT240100030

Abstract

Lifestyle variables, including physical activity and diet, are key determinants of bone remodelling. However, remodelling is also spatially limited by the anatomical form of bone. The extent to which these macroscopic, microscopic and lifestyle variables co-vary allometrically in humans is subject to ongoing investigation. We hypothesised that femur midshaft size and biomechanical properties would have a dimensional effect on the size and density of secondary osteons produced during remodelling, independently of age and sex, and that this effect would manifest under different lifestyle conditions. We examined femur midshaft microradiographs in 73 samples part of the Melbourne Femur Research Collection (Australia). We measured cortical/total area (CA/TA) and the ratio of axes of the largest and smallest femur rigidity areas (I_{max}/I_{min}); secondary osteon area (On.Ar), the ratio of Haversian canal to On.Ar (H.Ar/On.Ar), and total population density of intact and fragmentary (partially remodelled) secondary osteons (OPD) from the anterior, posterior, medial and lateral anatomical femur axes. Out of all the bone parameters, CA/TA and H.Ar/On.Ar showed low to high negative correlations ($p < 0.001$, r range −0.323 to −0.752) and negative allometry relationships in the entire sample, in males and in a sub-group that consisted of individuals who were sedentary but well nourished. In these groups, higher log values of CA/TA were associated with smaller log values of H.Ar/On.Ar, which translated to femoral midshafts with thicker cortices having less porous secondary osteons (smaller Haversian canals relative to thicker lamellar bone). However, this relationship was not evident in females and other age and lifestyle groupings. We suggest that effects of allometry on bone histology, or even basic variables such as cortical thickness, are included in future remodelling and lifestyle assessments to ensure that histological interpretations are not confounded by bone size.

KEYWORDS
bone histomorphometry, bone remodelling, cortical bone, cross-sectional geometry

1 | INTRODUCTION

Many factors influence human bone remodelling, the process of bone resorption and deposition, including those that comprise our daily lifestyles (Sheng et al., 2021). Apart from intrinsic biological variables, external key influences on bone remodelling can be exerted through variation in physical activity, diet and behaviours such as regular smoking and alcohol consumption (Proia et al., 2021; Sahni & Kiel, 2015). Understanding metabolic bone diseases where the mechanism at fault is an imbalance in bone resorption and deposition, such as osteoporosis, thus presents a complex investigation where multiple co-varying variables are at play. Another aspect, less considered in bone remodelling research than lifestyle, is the natural variation in anatomy and morphology observed in the human skeletal system, which can have a corresponding structural effect on the manifestation of microscopic bone products, called secondary osteons, created during and following remodelling by the Basic Multicellular Units (BMUs).

In cortical bone, BMUs produce longitudinal secondary osteons which are composed of concentric lamellae that envelop Haversian canals and are delimited from the surrounding bone by cement lines (Chang & Liu, 2022). Secondary osteons are roughly circular in shape when viewed in a transverse plane, although they show variation in this circularity in humans (Cooke et al., 2022). Secondary osteons are important in determining adult cortical bone mechanical and structural integrity (Chen et al., 2022) along with a key metabolic role of calcium, nutrient and oxygen exchange and supply to bone tissue (Forriol & Jedrzejczak, 2023). Their formation is entirely executed by BMUs which ultimately determine the final secondary osteon shape, size and proportions of lamellar bone to canal space (Doube, 2022). The larger the canal space, the higher the bone cross-sectional porosity (adding to other pores of non-Haversian origin). In relative terms, the quantity of lamellar bone deposited within a secondary osteon is dependent on osteoblast activity, whereas the extent of secondary osteon boundaries depends on osteoclast mediated resorption. This balance can be disturbed in osteoporosis. Primary osteons, which are later replaced by secondary osteons, form during modelling as bone size increases during growth (Allen & Burr, 2019). Whether human secondary osteon size forming during remodelling could be determined by the size of the bone it is being formed in is subject to ongoing investigation.

In transverse plane, a cross-section of a secondary osteon mirrors a long bone cross-section at midshaft. Both show central space surrounded by layers of bone tissue. Coincidentally, long bone cross-sections in lab rats and mice have been colloquially termed 'super osteons' due to their morphological similarities and mechanical competencies to secondary osteons (Goodyear et al., 2009; Koh et al., 2024). Each secondary osteon can be viewed as an independent functional unit with its own biomechanical properties determined through variation in collagen fibre orientation within individual lamellar layers (Skedros, 2024). Highly strained cortical bone regions can develop higher densities of secondary osteons in an attempt to provide further regional mechanical competence (Skedros et al., 1994, 1996). There should be, however, limited space within long bone cortical walls that varies across mammals so there is an evolutionarily underpinned anatomical limit to which secondary osteon size can continue expanding. As bone size across different taxa is genetically and functionally determined, skeletons of different sizes must balance nutrient delivery and blood flow through bone while maintaining bone strength and mechanical viability (Cowin & Cardoso, 2015). Because bone remodelling, and thus secondary osteon size and density, can vary with disease and lifestyle, it is important to understand the extent to which such inherent anatomical dimensional relationships might impact remodelling in these contexts. Our study investigates this concept by analysing scaling between human midshaft femur cortical bone biomechanical and size properties, and the corresponding size (see further below for definitions) and density of secondary osteons.

1.1 | Bone size-histomorphometry relationships in humans and other mammals

Allometric relationships at the tissue and microstructure level can be studied using allometric approaches that are evolutionary (across taxa), static (intra-specifically at the same/similar developmental stage) and ontogenetic (intra-specifically across different developmental stages) (Cheverud, 1982; Pélabon et al., 2014). Few studies have addressed direct allometry between various bone histology and bone size parameters in humans, but general relationships/correlations have often been reported. In the 1960s, in a study of nine mammalian species that included humans, Jowsey (1966) made some preliminary observations that smaller species (measured through approximate body weight) tend to show smaller secondary osteon and Haversian canal area. Jowsey's (1966) human sample included 26 adults where cortical thickness was also measured in the rib and the femur. Jowsey's (1966) data for secondary osteon diameter, calculated from an average of two perpendicular diameters measured between the cement line, and Haversian canal perimeter, appeared to be in a negative relationship with cortical thickness such that higher cortical thickness was associated with smaller histomorphometric values. Because Jowsey (1966) included humans up to 90 years old, thinner cortices reflected endosteal thinning with age. Mishra (2009), and Mishra and Knothe Tate (2004), analysed published data, including those from Jowsey (1966), to report positive allometry in secondary osteon area and Haversian canal perimeter with body weight across different mammalian species, including humans. Mishra (2009) discussed the importance of allometry from the perspective of evolutionary and metabolic advantage in the optimisation of secondary osteon and canal size supporting biotransport in bone tissue so nutrient supply is similar across different species.

In tibiae from human male donors, Ural and Vashishth (2006) found that secondary osteon area (total area of secondary osteons per given bone region and averaged individual secondary osteon area) in the distal mid-diaphysis was in a positive association with measures such as subperiosteal area, cortical area, principal and

polar moments of inertia. In a comparison between slender and robust bones, Goldman et al. (2014) noted that tibiae from human cadavers had more and larger secondary osteons (measured through total secondary osteon area) associated with bone robustness (total cross-sectional area/total tibial length), suggesting that there might be a global bone signal that modulates localised remodelling. In ribs from 80 human donors, Dominguez and Agnew (2016) found that area of secondary osteons (averaged per bone region) varied between different rib cortices, with the thicker pleural region of the rib cortex having larger secondary osteons. Miszkiewicz and Mahoney (2019) examined >400 femora of archaeological humans for allometry in midshaft histology, cortical thickness and robusticity indices (midshaft circumference/maximum femur length) to find negative allometry in secondary osteon area, Haversian canal area and diameter (which were averages per examined bone region). They noted that as bone robusticity increased and cortical thickness widened, secondary osteon and Haversian canal area became smaller.

Among non-human mammals, Felder et al. (2017) identified negative allometry in femoral and humeral secondary osteons with body mass spanning taxa that weighed between 300 g and 21,000 kg. They suggested that secondary osteon and Haversian canal area depend on mammalian size such that bones in smaller (measured through weight) species do not experience frequent fracturing, whereas larger species can sustain osteocyte viability. Paine and Godfrey (1997), in their study of the non-human primate femur and humerus, spanning 107 specimens representing Galagonidae and Cercopithecidae, found positive allometry in total secondary osteon area and bone cross-section area. While in this study total secondary osteon area, combining intact and partially remodelled secondary osteons, was used instead of areas of individual secondary osteons, it noted an obvious confounding variable of mechanical usage whereby their allometric coefficients varied depending on the fore- or the hind-limb and the taxon considered. Skedros et al. (2013) situated allometric analyses of Haversian canal to secondary osteon area ratios within the rib and the femur (in addition to the calcaneus, in a range of humans and other mammals). They tested the hypothesis that a bone such as the rib, which is deemed more metabolically optimised than a bone such as the femur (which receives higher and more variable mechanical loading than the rib), should show positive allometry in Haversian canal and secondary osteon area ratios. They found both positive and negative allometry results across the sample, but importantly, often found the opposite allometry to what had been hypothesised/expected. Most rib groups and limbs showed positive allometry, even though negative allometry had been expected for the limbs.

1.2 | Absence of bone size-histomorphometry relationships

While the above studies indicate allometry or general correlations in various measures of skeletal or body size, and secondary osteon size parameters, there have been other studies where this relationship was not evident. For example, a lack of correlations between secondary osteon population density and mean secondary osteon area in the human rib was noted between body mass and size (measured through skeletal morphometry) by Beresheim et al. (2018). In growing macaques, secondary osteon remodelling dynamics (measured through variables such as secondary osteon density and mean secondary osteon area) occurred irrespective of body weight (Burr, 1992). In humans, stature did not link with femur histological variables (secondary osteon area, diameter and circularity), but weight did (Britz et al., 2009). Zedda and Babosova (2021) compared femoral and humeral robustness indices and secondary osteon and Haversian canal area, perimeter, minimum and maximum diameters, finding that the ca. 10-fold difference in weight between cows and sheep did not significantly impact histological structures. Compared to the studies discussed earlier where these relationships were observed, there are some methodological points that may explain these contradictory findings, including small sample size ($n = 11$ cows, $n = 11$ sheep) in Zedda and Babosova (2021) and the use of the rib in Beresheim et al. (2018), which is likely to have different remodelling responses to body mass than limb bones.

1.3 | Developing bone size-histomorphometry allometry hypotheses

Considering the above findings where there might be an effect of bone size on histological parameters, there is a handful of papers published where secondary osteon and Haversian values are adjusted by bone size to account for variation in anatomical morphology, assuming a negative allometric relationship (e.g. Basilia et al., 2023; Miszkiewicz et al., 2023; Miszkiewicz & Mahoney, 2019; Miszkiewicz & van der Geer, 2022; Pedersen et al., 2024), but this is not common and begs the basic question of whether cross-sectional size of long bones can 'direct' cross-sectional size of secondary osteons that are forming within.

We tested the hypothesis that a relationship between macroscopic (cross-sectional size and shape) and microscopic (histological parameters) features of bone is present, using a documented human autopsy sample. We further used allometric analyses to characterise the nature of this relationship, to assess whether long bone cross-sectional size and secondary osteons generated during cycles of remodelling show positive, isometric or negative allometric relationships. We developed hypotheses which use different measures of secondary osteons: average secondary osteon area (On.Ar), average ratio of Haversian canal to secondary osteon area (H.Ar/On.Ar) (Figure 1) and the density of secondary osteons (osteon population density, OPD), per mm^2. We use the ratio size parameter because secondary osteons cannot only be understood through their overall area (resorption space). They have functional importance where a secondary osteon with a thicker lamellar wall offers better structural integrity (lower porosity), but a secondary osteon with a thinner lamellar wall improves vascularity and metabolic activity (higher porosity) (Figure 1). Our hypotheses are summarised in Table 1, and

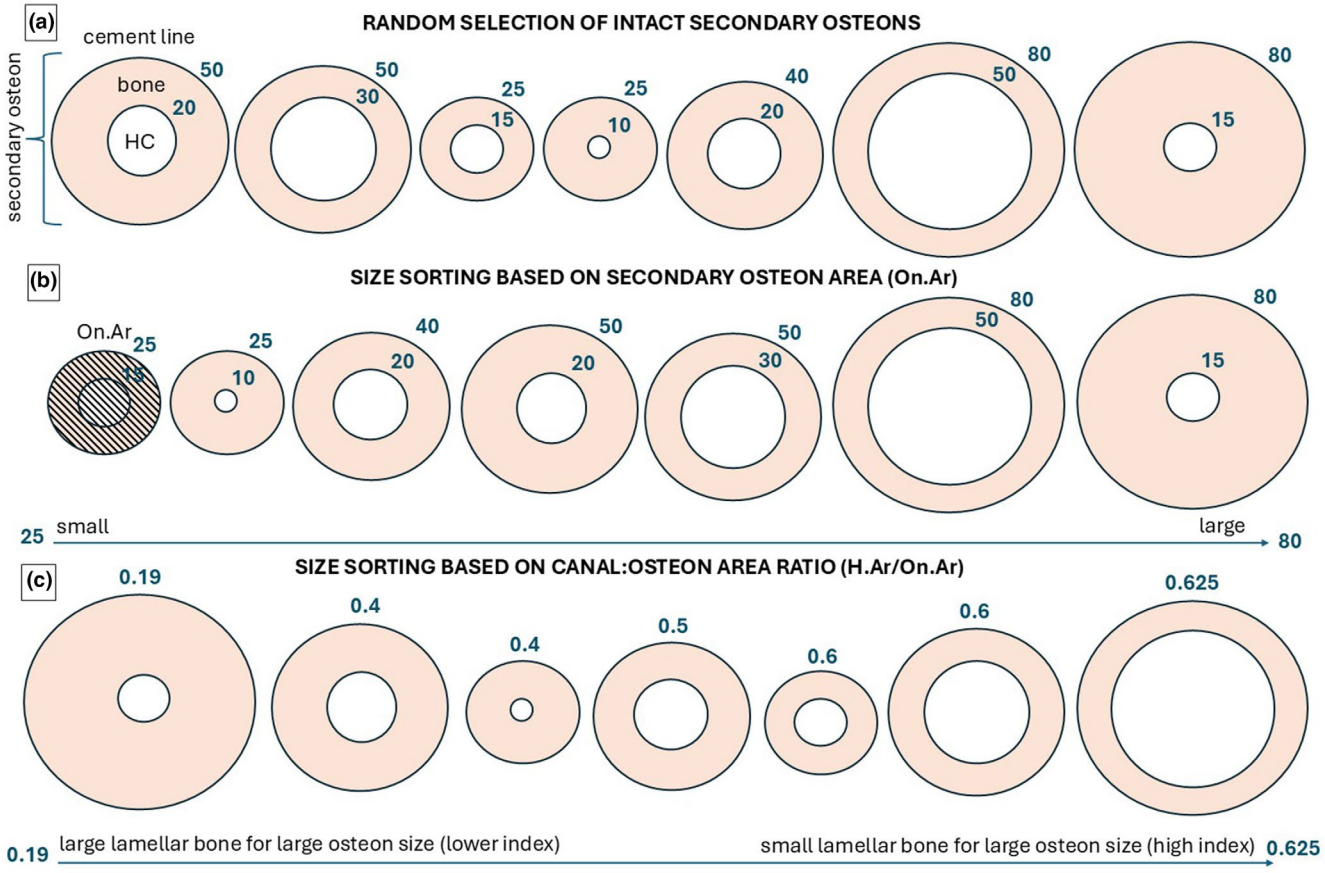

FIGURE 1 Diagram illustrating sorting based on absolute and relative size measures of secondary osteons. (a) shows a hypothetical randomly selected sample of secondary osteons that vary in their size both overall and in terms of their Haversian canals (HC). The values placed outside the cement line and the boundary of each Haversian canal are hypothetical only and on a 0–100 scale for ease of illustration of area measures. (b) illustrates sorting these secondary osteons based on overall area only. The black diagonal lines indicate the areas include in the total area calculation, which are the Haversian canal area and the area occupied by lamellar bone. (c) shows sorting based on the ratio calculated as Haversian canal area/secondary osteon area.

partially illustrated in Figure 2. If these allometric relationships are a result of inherent anatomical characteristics, we expect them to exist independent of age, sex and lifestyle (they should manifest in the same way in different groups).

2 | MATERIALS AND METHODS

This study uses human femoral cross-sections from autopsies of accidental deaths that occurred in Melbourne, Australia, during the late 1980s and early 1990s. To conduct this research, we received ethics clearance at the Australian National University (Protocol 2019/039) and the University of Melbourne (Melbourne Dental School HEAG 1955329, 1954534). Mortuary staff at the Victorian Institute of Forensic Medicine handling the autopsies extracted midshaft femoral blocks and fixed them in 70% ethanol (Thomas et al., 2005). These were later incorporated into The Melbourne Femur Research Collection (MFRC) at the University of Melbourne, Australia. Detailed sample preparation steps are reported in Thomas et al. (2005). Briefly, the sample of sections dedicated for histology was cleaned and had further ~0.3 mm thin slices sawn off using a Leitz 1600 sawing microtome. Following lapping on 1200 grit paper, the final thickness of each section was 100 μm. Some sections were imaged using microradiography and digitised to examine bone histology relationships with age, sex, weight and height (Britz et al., 2009; Thomas et al., 2005). The microradiography was carried out using a Matchlett Laboratories OEG X-ray tube, and the resulting microradiographs were mounted on glass slides for imaging on a Leitz Dialux 20 microscope fitted with a Diagnostic Instrument's Spot 2 camera (resolution of 1315 × 1033 pixels) (Thomas et al., 2005). Each image from a cross-section was montaged using Optimas macro language software. In our study, we worked with the images of microradiographs catalogued in the MFRC database.

The MFRC consists of more than 900 samples, but only a portion of the database includes digital microradiographs from the midshaft femur. We first screened the MFRC catalogue to randomly select $n = 75$ individuals ensuring they represent four age and sex sub-groups of young males, young females, middle-aged males and middle-aged females. We avoided the selection of

TABLE 1 Summary of our hypotheses.

Hypotheses	On.Ar higher values = larger secondary osteon (resorption area)	H.Ar/on.Ar lower values = relatively larger lamellar bone content for secondary osteon size	OPD higher values = more secondary osteons per mm^2	CA/TA higher values = relatively thicker cortical bone	I_{max}/I_{min} ≤1 = midshaft circular and stronger in all directions, >1 = midshaft elliptical & stronger anteroposteriorly	Interpretation
Positive allometry data predictions						
Hypothesis A based on On.Ar	↑	n/a	n/a	↓	<1	Secondary osteons grow larger relative to thinner midshaft cortex
Hypothesis B based on H.Ar/On.Ar	n/a	↑	n/a	↓	<1	Secondary osteons are more porous for relatively thin cortex
Hypothesis C based on OPD	n/a	n/a	↑	↓	<1	There are more secondary osteons relative to thinner midshaft cortex
Isometry data predictions						
Hypothesis A based on On.Ar	1	n/a	n/a	1	1	Secondary osteons and midshaft cortical bone change at the same rate
Hypothesis B based on H.Ar/On.Ar	n/a	1	n/a	1	1	
Hypothesis C based on OPD	n/a	n/a	1	1	1	
Negative allometry data predictions						
Hypothesis A based on On.Ar	↓	n/a	n/a	↑	>1	Secondary osteons grow smaller relative to thicker midshaft cortex
Hypothesis B based on H.Ar/On.Ar	n/a	↓	n/a	↑	>1	Secondary osteons are less porous relative to thicker midshaft cortex
Hypothesis C based on OPD	n/a	n/a	↓	↑	>1	There are fewer secondary osteons relative to thicker midshaft cortex

elderly individuals because they are likely to experience osteoporosis due to advanced age. The young group (average 27.5 years old, range of 20–35 years old) was targeted as it is when the peak bone mass accrual occurs. The middle-aged group had an average of 42.5 years old (range of 36–50 years old) covering perimenopause and possibly menopause (Greendale et al., 1999). Therefore, the conditions of the sample screen were (1) age, (2) sex, (3) availability of the microradiographs and (4) availability of autopsy questionnaires and pathologist's comments on the condition of the autopsies. All the samples were blinded during the data collection. Upon unblinding, we identified that two individuals were of Asian ancestry, while the remainder of the sample was

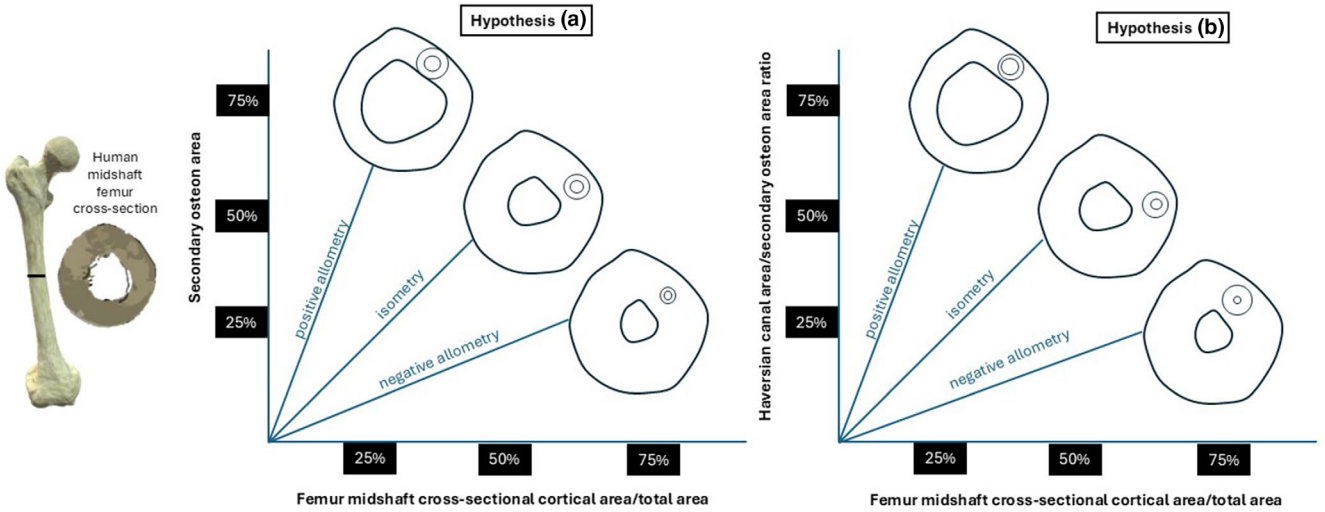

FIGURE 2 Two (of three, C is not illustrated, see Table 1) scaling hypotheses developed in our study based on secondary osteon area (a) and the ratio of Haversian canal area and secondary osteon area (b) (see Table 1 for secondary osteon population density). In Hypothesis A, secondary osteons grow larger relative to thinner midshaft cortex if there is positive allometry; secondary osteons and midshaft cortical bone change at the same rate if there is isometry; or secondary osteons grow smaller relative to thicker midshaft cortex if there is negative allometry. In Hypothesis B, secondary osteons are more porous for relatively thin cortex if there is positive allometry, secondary osteons and midshaft cortical bone change at the same rate if there is isometry; or secondary osteons are less porous relative to thicker midshaft cortex if there is negative allometry.

Caucasian. The two samples of Asian ancestry were excluded to reduce ancestry-related heterogeneity. This methodological approach resulted in a total sample size of $n = 73$ with $n = 34$ females and $n = 39$ males. The age and sex distribution of the entire sample are shown in Table S1.

While all causes of death were accidental, we also checked for any bone-related conditions or injuries that might have impacted the individuals' ability to use their lower limbs and thus influence secondary osteons seen in the microradiographs at the time of death. Any major conditions would have also been filtered out and the case excluded before collection. Almost all individuals in our study were noted to have no skeletal or musculo-skeletal conditions, except for items such as 'normal osteoporosis' or 'osteoporosis compatible with age' (5.5% of individuals). Other conditions commonly noted included fractures of the ribs and the skull (~25% of individuals), which we decided to retain since they were not related to limbs. Although weight and height are also available in the database, we decided to exclude them as they are measures taken at the time of death not reflecting true measures when alive.

Next-of-kin autopsy questionnaires and pathologist's notes from autopsies were reviewed to seek and extract descriptions of each individual's condition and information about occupation, if available. This information includes comments on build (such as height, robustness, slenderness, gracileness, weight/overweight/obesity), dietary tendencies and other habitual factors such as alcohol drinking, smoking and generic physical activity sometimes specifically referring to whether occupations were sedentary or active. As there was inconsistency in the way these were reported for each individual, this information was extracted qualitatively first into a spreadsheet and later examined using a standard thematic analysis approach identifying trends that allowed for categorisation into lifestyle groupings (Clarke & Braun, 2017). This involved extracting keyword/s and assessing the entire sample for repeated occurrences of the same or similar keyword/s. We then coded any keyword repetitions, which allowed us to quantify them and organise into categories that ultimately grouped individuals of the same or similar body characteristics. We cannot provide the exact keywords recorded to protect the identity of our subjects, but we were able to generate at least four usable groupings based on these keywords (Table 2). Sixteen individuals remained uncategorised due to a lack of usable data in the autopsies and next-of-kin reports. This group, along with group 4 (active, poorly nourished) with low sample size, had to be excluded from the lifestyle component of analyses in the present study.

2.1 | Derived bone variables

We included five main bone variables in this study, two of which measured biomechanical properties of the midshaft femur that translate cross-section size, and three of which were secondary osteon parameters per region of interest (ROI). Table 3 summarises these variables and definitions, and they are also illustrated in Figures 3 and 4.

2.1.1 | Cross-sectional geometry

Two cross-sectional variables were derived using four initial individual variable measurements made from the midshaft femur images using

TABLE 2 Lifestyle groups based on next-of-kin verbal autopsy questionnaires and pathologist autopsies representation in the sample.

Lifestyle groups	*n*
0 = uncategorised (no useable data in autopsies, next-of-kin reports)	16
1 = ordinary (nothing unusual or extreme noted)	25
2 = active, well nourished (comments specific to being physically active and consuming a balanced diet)	15
3 = sedentary, well nourished (comments specific to not being physically active but consuming a balanced diet)	11
4 = active, poorly nourished (comments specific to being physically active with unhealthy diet tendencies)	1
5 = sedentary, poorly nourished (comments specific to not being physically active with unhealthy diet tendencies)	5

Note: In brackets are general definitions capturing the information contained in those reports without revealing specific terms to protect individual identity.

TABLE 3 Five bone variables examined in our study and their definitions.

Methods	Derived variables	Abbreviation	Definition	Ref.
2D cross-sectional geometry from digitised femur micro-radiographs	Ratio of maximum and minimum principal axes or moments of inertia	I_{max}/I_{min}	Ratio of maximum and minimum principal biomechanical axes across midshaft femur which indicate the largest and smallest, distributions of mass, respectively	For example, Feik et al., 2000; Stock & Shaw, 2007
	Proportion of total area comprised of cortical cross-sectional area	CA/TA	Proportion of cortical area relative to total area of femur midshaft cross-section, reflecting the proportion of bone within the femur midshaft	For example, Miszkiewicz et al., 2022; Ruff, 2018
2D histomorphometry from digitised femur micro-radiographs	Secondary osteon area	On.Ar	The area of resorption by BMUs delimited by a cement line, including the space occupied by its central Haversian canal. This is an absolute size measure of the secondary osteon	For example, Britz et al., 2009; Skedros et al., 2013
	Proportion of Haversian canal area relative to secondary osteon area	H.Ar/On.Ar	Proportion of the area in transverse plane occupied by a Haversian canal within a secondary osteon relative to the entire area of the same secondary osteon (measured by tracing the cement line), indicating the relative quantity of lamellar bone contained with the secondary osteon. The higher the value the thinner the bone space in the secondary osteon	For example, Cooke et al., 2022; Miszkiewicz & Mahoney, 2019
	Secondary osteon population density	OPD (#/mm^2)	A total number of secondary osteons seen within a region of interest made up of intact (not remodelled) and fragmentary secondary osteons (partially remodelled) divided by the ROI area. Secondary osteons cut off by ROI border are excluded from counts	For example, Frost, 1987; Stout & Paine, 1994; Matsuo et al., 2019

standard methods in long bone cross-sectional geometry (Gosman et al., 2013; exact method is described in Miszkiewicz et al., 2022). The individual variables were total area (TA), cortical area (CA), and maximum and minimum principal axes or moments of inertia (I_{max}, I_{min}), which were converted into proportions as CA/TA and I_{max}/I_{min} (Ruff, 2018). Higher CA/TA values indicate thicker cortical wall, whereas higher I_{max}/I_{min} values (>1) indicate a cross-section that is more elliptical and stiffer along the anteroposterior axis (closer to 1 means the cross-section is more circular). These measurements were obtained using the BoneJ plugin of FIJI/ImageJ (Doube et al., 2010; Schindelin et al., 2015). Prior to measurement, images were imported into FIJI/ImageJ where they were cropped and had the background cleared to only show the femur section using the 'clear outside' and 'clear' function applied to an area measurement circled using the 'freehand line' tool. The image was then converted to 16-bit and the threshold function was applied to binarise the image and fill any voids. The data for I_{max} and I_{min} were obtained from axes calculated using the 'slice geometry' option in FIJI/ImageJ (Doube et al., 2010).

2.1.2 | Cortical bone histomorphometry

At their original capture in prior MFRC projects, the femur microradiographs were calibrated using individual tiles of 576 height × 512 width in pixels (approximately 3.56 × 2.67 mm per tile). These pixels were converted into mm in FIJI/ImageJ. Regions

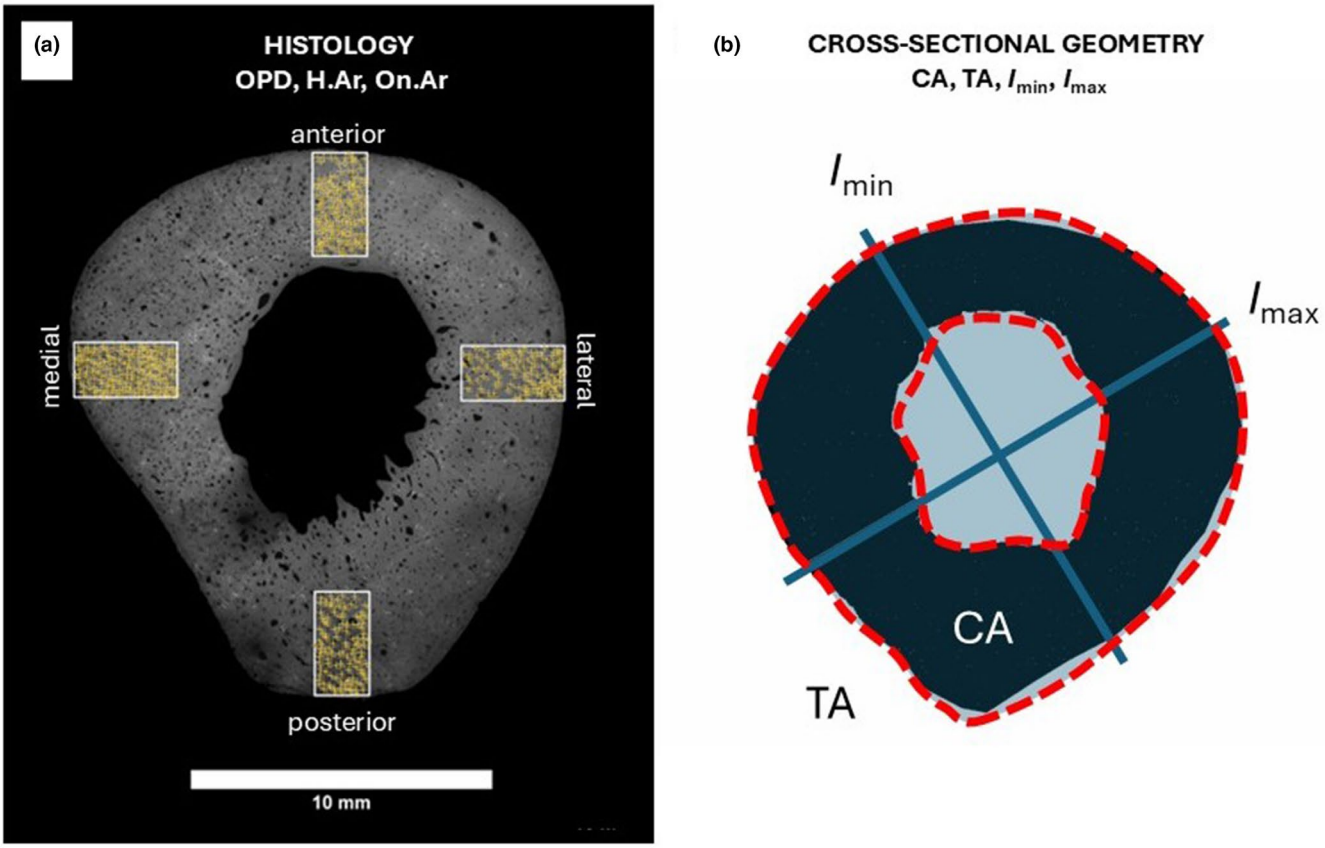

FIGURE 3 Illustration of bone analysis methods applied in our study. (a) shows a microradiograph of one of the Melbourne Femur Research Collection femoral midshaft segments. The four rectangles placed on the anterior, posterior, medial and lateral axes are regions of interest from which secondary osteon population density (OPD), Haversian canal (H.Ar) and secondary osteon (On. Ar) area were measured. (b) shows a cross-section of another MFRC femoral midshaft segment that had been converted to black and white and had threshold analysis applied in FIJI/ImageJ hence the black only filling of the cortical wall. These images were analysed for cross-sectional geometry with I_{max} and I_{min} indicated with straight purple lines, total area (TA) with light purple shading covering the cortical space and the medullary space and cortical area (CA) boundaries indicated with the red dashed lines. Cross-sectional properties shown in (b) are drawn for illustrative purposes only.

of interest were manually applied in FIJI/ImageJ by selecting the 'rectangle' tool and specifying its dimensions to 1.8 mm by 3.42 mm. The size of the ROI was determined based on the recommendation by Stout and Crowder (2011) that a minimum of 25 secondary osteons should be measured per sampled region. Because our overall sample includes young individuals with sparser secondary osteons than in older individuals, we needed to ensure a wide enough ROI to capture enough secondary osteons. Each ROI was placed starting at the sub-periosteal region along each of the anatomical axes (anterior, posterior, medial, lateral). From within the ROI, the collected parameters were intact secondary osteon number, fragmentary secondary osteon number, secondary osteon area and Haversian canal area. The secondary osteon counts were summed to create a total secondary osteon number, which was then divided by the ROI area to yield the calculation of osteon population density. The counts were performed manually using the 'multi-point' tool in FIJI/ImageJ, and any secondary osteons cut off by the ROI border were excluded. The area values for both the Haversian canals and secondary osteons were taken using the 'freehand' tool in FIJI/ImageJ by tracing the border of the canal and the cement line and averaged for each individual. The area of secondary osteons (On.Ar) was used as an absolute measure of secondary osteon size. A relative measure was computed as H.Ar/On.Ar using the averages of On.Ar and area of Haversian canals (H.Ar). Only intact secondary osteons and canals were measured, that is, no primary osteons or secondary osteons that had been partially remodelled (fragmentary). The H.Ar/On.Ar parameter gives a measure of secondary osteon size that is not confounded by Haversian canal area. Further, when we refer to a secondary osteon area as 'large' or 'small', we mean that the absolute values are increasing, while the relative values are decreasing where there are large amounts of lamellar bone present per large area (Figure 2). We will use the terms 'large' versus 'small' when referring to On.Ar only (see panel B in Figure 2), and 'large bone content for large midshaft' versus 'small bone content for large midshaft' when referring to H.Ar/On.Ar. From this perspective, secondary osteons that are large based on On.Ar only can include both those that have thick lamellar walls and those that have large central pores. The H.Ar/On.Ar parameter, on the other hand, will allow to distinguish the different morphologies of secondary osteons through a lower versus higher ratio value, respectively.

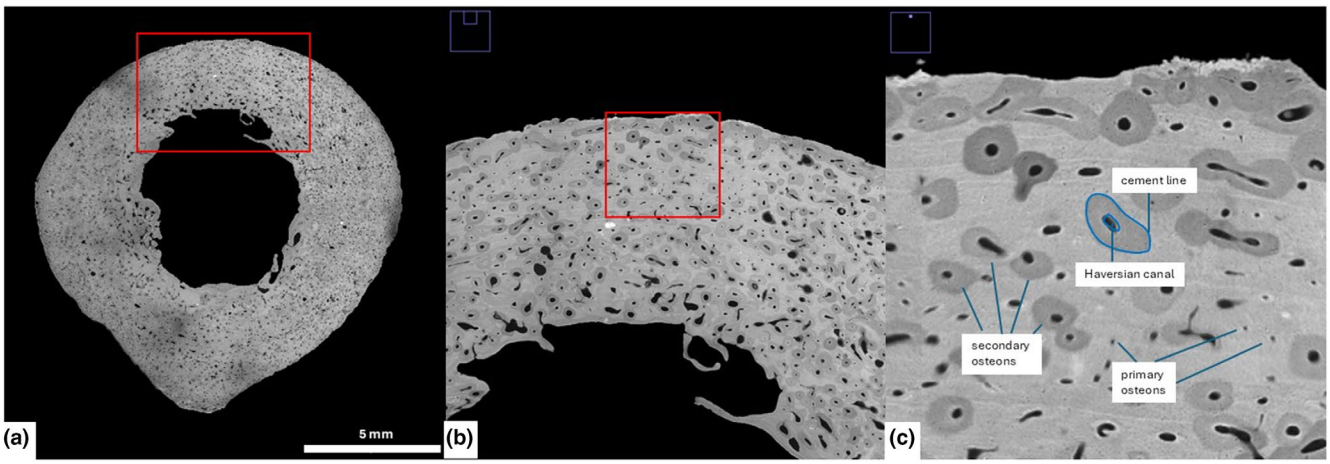

FIGURE 4 Example of a microradiograph from the MFRC collection viewed in its entirety (a) and then with a close up on the anterior region (b), and further close up showing osteonal elements, such as secondary osteons (also indicated through the cement line and containing a Haversian canal), and primary osteons (c). Our study only worked with secondary osteons which result from remodelling processes.

2.2 | Statistical analysis

First, all data were examined descriptively by reviewing mean data and initial observations about data variation were made. Prior to selecting statistical tests, we examined data normality through Shapiro–Wilk tests where it was identified that On.Ar, H.Ar/On.Ar and OPD were normally distributed (Table S2). Because we undertook multiple testing, we adjusted the p value with a Bonferroni correction ($p < 0.0125$). Second, we ran a 'background' analysis essential in double checking that our data did not differ statistically between ages, sexes and lifestyles to allow for allometric analyses, in addition to exploring potential relationships between On.Ar and H.Ar/On.Ar. The test for group differences was a t-test (with I_{max}/I_{min} and CA/TA log transformed), a Kruskal–Wallis when comparing lifestyle groups between 1 and 3 lifestyle groups (where sample size warranted statistical analysis) and a Pearson's r correlation for the On.Ar and H.Ar/On.Ar relationship (with Spearman's Rho used in Lifestyle groups 2 and 3 where $n < 20$). Multiple correlations were additionally explored between the histology variables only to check how they related to one another through Pearson's r and visualised through a correlogram. We also performed a multivariate linear regression with one independent (CA/TA) and three dependent histology variables (On.Ar, H.Ar/On.Ar and OPD) to see which one or more than one histology measures changed in response to CA/TA changes. When interpreting the strength of correlation coefficients, we followed the Hinkle et al. (2003) recommendations where positive or negative r values are deemed: negligible ($r = 0.00–0.30$), low ($r = 0.30–0.50$), moderate ($r = 0.50–0.70$), high ($r = 0.70–0.90$) and very high ($r = 0.90–1.00$).

To test our hypotheses outlined in scenarios A–C, we log-transformed the rest of the data and analysed it using a reduced major axis regression (RMA). We chose to use the RMA because it allows for some error in the x and y variables, which we could expect in the histology, femoral cross-sectional geometry and biomechanical measures (Smith, 2009). Isometry was identified when/if slope $b = 1$. When/if $b < 1$ or >1, negative or positive allometry was identified, respectively, along with 95% confidence intervals that included values ≤1 (negative) and >1 (positive). We ran the RMA tests sub-dividing the sample by sex and age groups first and then comparing lifestyle groups where possible. For the latter, this includes the lifestyle group 3 where $n = 11$ as RMA does not depend on large sample sizes and the slope estimation is unbiased by symmetry, although we will encourage cautious treatment of results for this group. For all analyses, we used IBM SPSS 30 and Past3 4.06b (May 2021 version). Our analysis takes the approach of static allometry measuring bone trait changes in a sample of individuals at the same stage of development (Pélabon et al., 2014).

3 | RESULTS

As can be seen from the descriptive data given in Table 4 (and further sub-group divisions in Table S3), the mean values of all the cross-sectional geometry and histology variables were similar across the age, sex and lifestyle groups. This was particularly obvious for all the ratios (I_{max}/I_{min}, CA/TA, H.Ar/On.Ar), whereas OPD showed slightly more variability, with it being the highest in the older age group when compared to the young (Table 4) and the older male sub-group when compared to younger males (Table S3). Secondary osteon area was also slightly smaller in the older than in the younger group (Table 4), but very similar when compared between the sexes.

When examining the descriptive data for the lifestyle groups, OPD also showed the highest values in: the sedentary and poorly nourished group overall (Table 5), in males and females separately (Table S4, although $n = 1$) and the younger age group (Table S5, although $n = 1$); and in the ordinary lifestyle group in the older age group (Table S5). The mean values for H.Ar/On.Ar were the highest in the active but poorly nourished lifestyle group (16.36, compared to 11.07–12.89 for all other groups, Table 5), though represented

TABLE 4 Descriptive data sub-divided by age and sex.

		N	Min	Max	Mean	SD
Sex						
F	I_{max}/I_{min}	34	0.45	0.99	0.79	0.12
	CA/TA	34	0.58	0.83	0.75	0.05
	On.Ar (μm^2)	34	15,460.42	43,665.25	25,427.72	5618.92
	H.Ar/On.Ar	34	7.20	16.57	11.42	2.14
	OPD (#/mm^2)	34	11.41	35.70	23.20	4.59
M	I_{max}/I_{min}	39	0.57	1.54	0.80	0.20
	CA/TA	39	0.44	0.90	0.73	0.08
	On.Ar (μm^2)	39	15,326.77	36,160.75	25,480.35	5512.90
	H.Ar/On.Ar	39	7.55	18.86	12.29	2.44
	OPD (#/mm^2)	39	16.98	35.17	23.12	4.59
Age						
20–35	I_{max}/I_{min}	40	0.54	0.99	0.76	0.11
	CA/TA	40	0.44	0.83	0.74	0.08
	On.Ar (μm^2)	40	15,460.42	43,665.25	26,466.31	6050.19
	H.Ar/On.Ar	40	7.20	18.86	11.40	2.37
	OPD (#/mm^2)	40	11.41	35.70	22.13	4.41
36–50	I_{max}/I_{min}	33	0.45	1.54	0.84	0.20
	CA/TA	33	0.52	0.90	0.74	0.07
	On.Ar (μm^2)	33	15,326.77	35,087.01	24,231.02	4606.02
	H.Ar/On.Ar	33	8.77	17.15	12.48	2.16
	OPD (#/mm^2)	33	17.31	35.17	24.40	4.49

by only one data point. Similarly to OPD, the mean values of On.Ar varied between the different lifestyle groups, showing the highest values in the ordinary group and the smallest in the sedentary, well-nourished group (Table 5; Tables S4 and S5).

Apart from some of this descriptive variability illustrated overall in Figure 5, there were no statistically significant differences in either the cross-sectional geometry or histology variables when comparing the sexes, age groups and lifestyle groups (Table S6).

Generally, there were some statistically significant correlations between the different histology variables. In particular, there was a statistically significant moderate negative correlation between On.Ar and H.Ar/On.Ar ($r = -0.541$, $p < 0.0001$, Figure 6), which was also the case across all the ages and sexes except the middle-aged sub-group and the lifestyle groups 2 and 3 (Table S7). There were also low and moderate negative correlations between OPD and On.Ar, but not H.Ar/On.Ar (Table S7, Figure S1). The multivariate linear regressions for CA/TA and histology measures of On.Ar, H.Ar/On.Ar and OPD yielded no consistently strong and statistically significant results, except for H.Ar/On.Ar in the entire sample, males and lifestyle group 3 that included sedentary but well-nourished individuals (Table 6; Table S8). This trend for these three sub-groups was also revealed in the RMA regressions once all the data were log transformed (Table 6, Table S9; Figure 7). Higher log values of CA/TA were associated with smaller log values of H.Ar/On.Ar, which translated to femoral midshafts with thicker cortices having less porous secondary osteons (smaller Haversian canals relative to thicker lamellar bone).

4 | DISCUSSION

Our study found negative allometry in the relationship between CA/TA human midshaft femur and H.Ar/On.Ar contained within. Our finding was such that femoral midshafts of higher CA/TA, which indicates thicker cortical wall, tended to produce less porous thick-walled secondary osteons (lower H.Ar/On.Ar value). This was clear across the entire sample, in males and within one specific lifestyle group that included individuals who would have had sedentary lifestyles but were well nourished. However, testing for allometry in other sub-groups of sex, age and lifestyle indicated low magnitudes of variation among the measured variables and resulted in no statistically significant findings, except for total density of secondary osteons within prescribed regions of interest. The latter finding, however, was also restricted to a small number of sub-groups. We will first briefly examine possible reasons behind the limited variation among parameters measured in our sample before discussing the significance of the identified allometric relationships.

Although we hypothesised that any inherent anatomical–histological relationships would be independent of age, sex and lifestyle, we still expected cross-sectional geometry and histology variables

TABLE 5 Descriptive data sub-divided by lifestyle groups based upon questionnaires and verbal autopsies (the 'uncategorised' group for 16 individuals is not shown).

Lifestyle		N	Min	Max	Mean	SD
Ordinary	I_{max}/I_{min}	25	0.62	1.48	0.81	0.17
	CA/TA	25	0.64	0.90	0.75	0.06
	On.Ar (μm^2)	25	18,011.24	36,160.75	26,789.57	5127.09
	H.Ar/On.Ar	25	8.40	16.57	11.07	1.94
	OPD (#/mm^2)	25	11.41	35.17	23.01	4.75
Active, well nourished	I_{max}/I_{min}	15	0.54	1.54	0.82	0.24
	CA/TA	15	0.44	0.83	0.73	0.10
	On.Ar (μm^2)	15	15,588.89	31,362.64	24,551.98	4474.84
	H.Ar/On.Ar	15	8.85	15.82	12.43	2.18
	OPD (#/mm^2)	15	17.73	30.04	22.78	4.00
Sedentary, well nourished	I_{max}/I_{min}	11	0.45	0.94	0.74	0.14
	CA/TA	11	0.52	0.80	0.71	0.09
	On.Ar (μm^2)	11	15,326.77	34,936.60	23,889.35	6034.55
	H.Ar/On.Ar	11	7.55	18.86	12.89	3.31
	OPD (#/mm^2)	11	17.03	28.68	23.88	4.30
Active, poorly nourished	I_{max}/I_{min}	1	0.82	0.82	0.82	n/a
	CA/TA	1	0.84	0.84	0.84	n/a
	On.Ar (μm^2)	1	24,155.590	24,155.590	24,155.590	n/a
	H.Ar/On.Ar	1	16.36	16.36	16.36	n/a
	OPD (#/mm^2)	1	18.06	18.06	18.06	n/a
Sedentary, poorly nourished	I_{max}/I_{min}	5	0.64	0.84	0.75	0.10
	CA/TA	5	0.66	0.78	0.72	0.04
	On.Ar (μm^2)	5	15,460.42	28,657.96	23,166.05	5619.83
	H.Ar/On.Ar	5	8.77	13.18	11.63	1.84
	OPD (#/mm^2)	5	21.32	35.70	26.51	6.17

would reflect some trends based on commonly occurring patterns in bone growth. For example, females often show higher bone porosity and smaller femoral midshaft measurements and biomechanical properties than males due to sexual dimorphism and hormonal changes related to reproduction and menopause (e.g. Bousson et al., 2001; Riggs et al., 2004; Šešelj et al., 2012). There have also been reports of secondary osteon size changing with age such that progressing age crowds secondary osteons, which physically constrains their area (Beresheim et al., 2018). Age might be a possible contributor to the small variability in OPD in our sample as its values were consistently the highest in the older group overall and when sub-divided by sex. This makes sense as we have known for decades that secondary osteon densities increase with age (Kerley, 1965), unless there are some disturbances to their formation such as malnutrition or extreme changes in mechanical signalling (Gocha & Agnew, 2016; Paine & Brenton, 2006). To this end, our OPD data were also the highest in the lifestyle group that we would predict to have the lowest secondary osteon densities—the sedentary and poorly nourished group. However, the sample size of one individual in two of these groups points to an age rather than diet or physical activity factor. Similarly, an unusually high mean H.Ar/On.Ar was noted in one individual in the active but poorly nourished group, indicating thin lamellar bone formed per secondary osteon which could be linked with the lifestyle status of the group. Despite all these points, the lack of statistically significant results makes our remarks cautious. Therefore, a more conservative explanation for our data would be that the sample was homogenous regardless of differences in age, sex, or activity. In comparison with previous studies which examined wider age ranges (e.g. samples from individuals aged between 29 and 93 years of age in Epelboym et al., 2012), highly structured social roles impacting activity (e.g. the differences in medieval status in Miszkiewicz & Mahoney, 2016) or the effects of past subsistence strategies on bone microstructure (Paine & Brenton, 2006), the results in our study show a highly homogenous population. When contrasted with more historical and ancient populations, our data for the recent Australian population, could be reflecting less variable physical activity in the last few decades.

The three statistically significant allometries between CA/TA and H.Ar/On.Ar follow our prediction of a macro–microscopic dimensional relationship. The shape similarity of a femur midshaft and secondary osteon cross-section is so striking that perhaps it is not a surprise that allometry does exist at this level. While we also noted

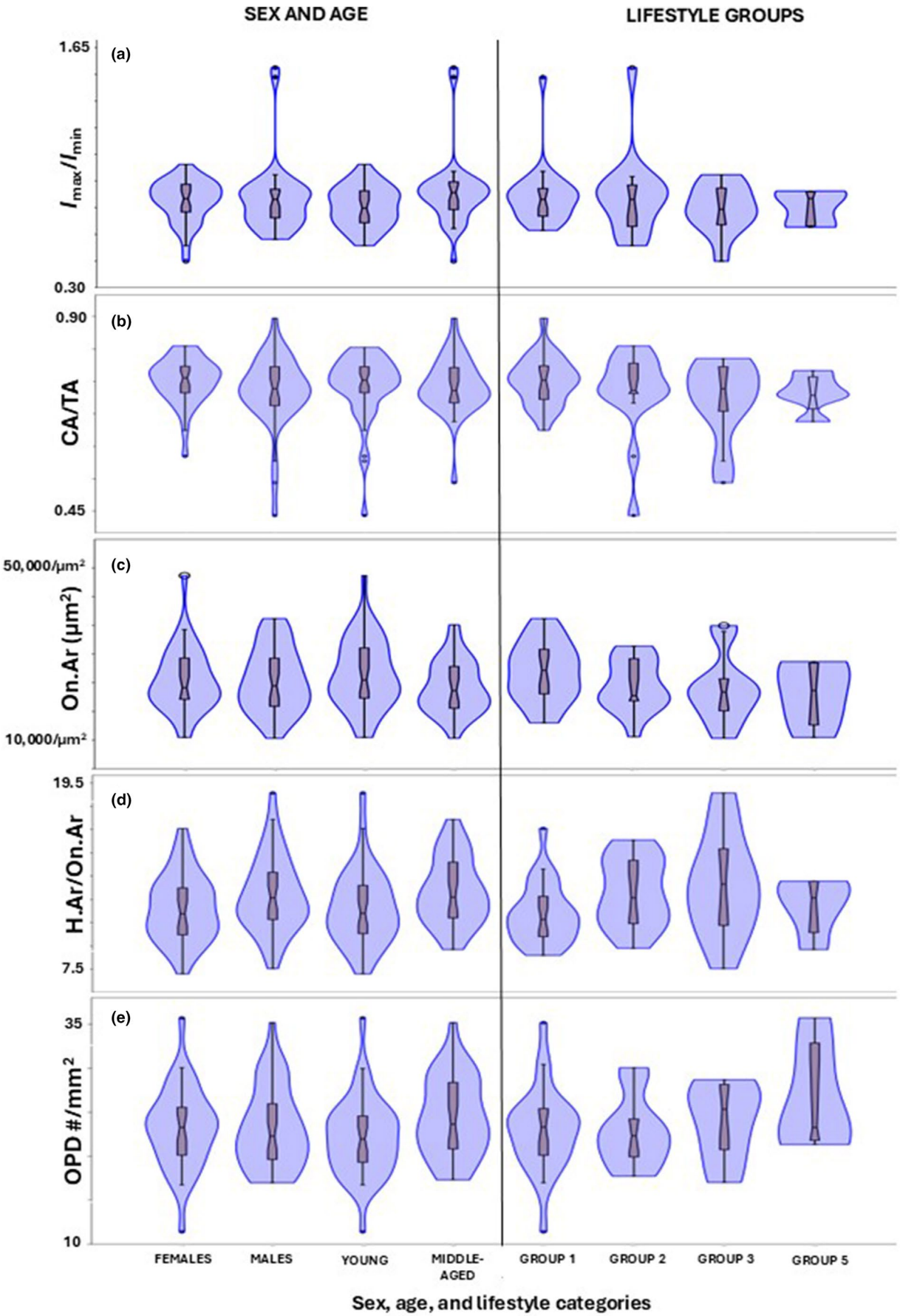

FIGURE 5 Violin and bar plots illustrating the cross-sectional and histology data across sex and age (left panel) and lifestyle groups (right panel). The circle and asterisks on the plots indicate outliers. The lifestyle groups are as follows: Group 1: Ordinary; group 2: Active, well nourished; group 3: Sedentary, well nourished; group 4: Active, poorly nourished (not shown due to $n=1$); group 5: Sedentary, poorly nourished. I_{max}/I_{min}, CA/TA and H.Ar/On.Ar are unitless as they are ratio values. I_{max}/I_{min}: Maximum and minimum second moments of area, CA/TA: Cortical to total area of midshaft femur cross-section, On.Ar: Secondary osteon area, H.Ar: Haversian canal area; OPD: Secondary osteon population density.

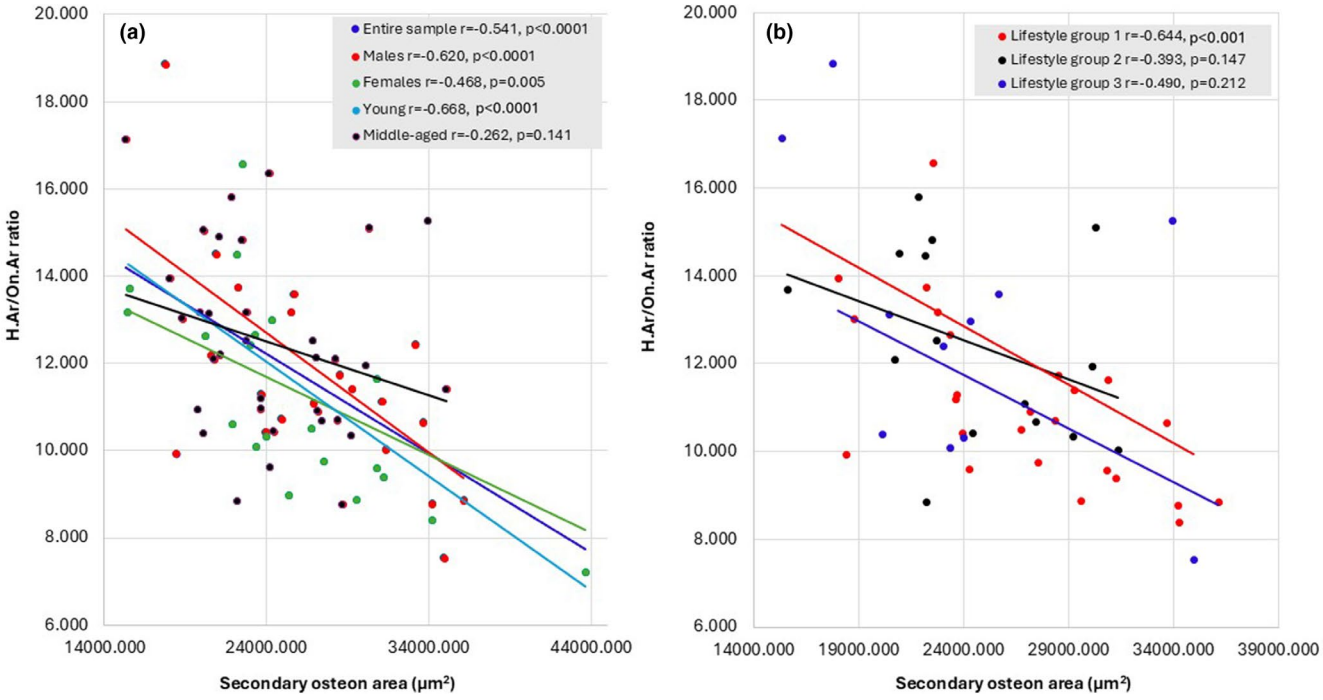

FIGURE 6 Scattergrams illustrating low and moderate (and one negligible) negative correlations between secondary osteon area and the ratio of Haversian canal area to secondary osteon area. Although they are not consistent, the highest coefficient of variation is −0.668 ($r^2=45\%$) for the young group. This shows that, on average, larger secondary osteon area is also associated with lower ratio values, meaning more bone content for secondary osteon size, in our sample.

a moderate negative correlation between On.Ar and H.Ar/On.Ar, which might signal that both are a good measure of secondary osteon size in our sample, the explained proportion of data was still not high (~45% in the highest *r*, Table S7; Figure 6) and On.Ar did not seem to correlate with CA/TA in the same way that H.Ar/On.Ar did. Our findings appear to correspond to negative allometries reported previously by Felder et al. (2017), where smaller Haversian canals were associated with larger mammals. While in that study, Felder et al. (2017) correlated body mass, not bone size or another measure of bone macrostructure, with bone histology and used a range of mammalian taxa, they did report that their findings appeared independent of phylogeny. Intra-specifically, our findings also agree with Miszkiewicz and Mahoney (2019) who worked with a large sample of archaeological human femora also running RMA tests and finding the same macro–microscopic relationships as us, except they only focused on the posterior aspect and used cortical thickness ('width') and a robusticity index calculated from this thickness and femur length, instead of a complete cross-section. They also reported that thicker and more robust femora (on the posterior aspect at least) tended to produce smaller secondary osteons with smaller Haversian canals. Since they worked with archaeological specimens, our study now confirms their findings on a modern documented human sample.

Since our results for the allometric relationships were clear in the entire sample and only two sub-groups (males and one lifestyle group), their lack of occurrence in the remainder of our sample subgroups warrants discussion. Given that only the males and not females were noted to have this allometry, sex-related bone metabolic processes appear to be a key factor in how the macro–microscopic relationships at the femur midshaft are expressed. This is consistent with well-established differences in how males and females experience remodelling at different points in their lifespan (Heaney et al., 2000). Females have additional biological pressures on their peak bone mass due to a series of sex-specific functions, such as reproduction (pregnancy and menopause) and lactation associated with high calcium needs and changing oestrogen levels (Grizzo et al., 2020; Mills et al., 2021; Ulrich et al., 2003). It is possible that the histology data for our females includes some individuals whose skeletal system was under such stress since we sampled adults aged >20 years and those in peri- and menopause ages 40–50 years old

TABLE 6 Results from the reduced major axis analysis for the entire sample, males and the lifestyle group of sedentary and well-nourished.

Multivariate linear regression	r^2	*p*	Mean squared error	MANOVA Wilks' lambda	*F*	df1 and df2
Males	0.097	0.005*	0.007	0.694	5.131	3 and 35
Slope and intercept	**Slope**	**Error**	**Intercept**	**Error**	***r***	***p***
Entire sample H.Ar/On.Ar	−0.583	0.203	0.989	0.029	−0.323	0.005*
Males H.Ar/On.Ar	−0.642	0.229	0.991	0.035	−0.418	0.008*
Lifestyle Group 3 H.Ar/On.Ar	−1.398	0.408	0.882	0.067	−0.752	0.008*
Reduced major axis regression with correlations	***r***	***p***	**Slope (*b*)**	**Intercept**	**Slope CI 95%**	***p***	**Relationship[a]**
Entire sample $CA/TA_{(log)}$ and $H.Ar/On.Ar_{(log)}$	−0.323	0.005*	−1.805	0.825	−2.348, −0.951	<0.0001	Negative allometry
Males $CA/TA_{(log)}$ and $H.Ar/On.Ar_{(log)}$	−0.418	0.008*	−1.5351	0.865	−2.034, −0.416	<0.0001	Negative allometry
Lifestyle group: sedentary, well nourished (Group 3) $CA/TA_{(log)}$ and $H.Ar/On.Ar_{(log)}$	−0.752	0.006*	−1.857	0.811	−2.642, 0.278	0.0014	Negative allometry

[a]$b > 1$: positive allometry, $b = 1$: isometry, $b < 1$: negative allometry.

*Bonferroni corrected $p < 0.0125$.

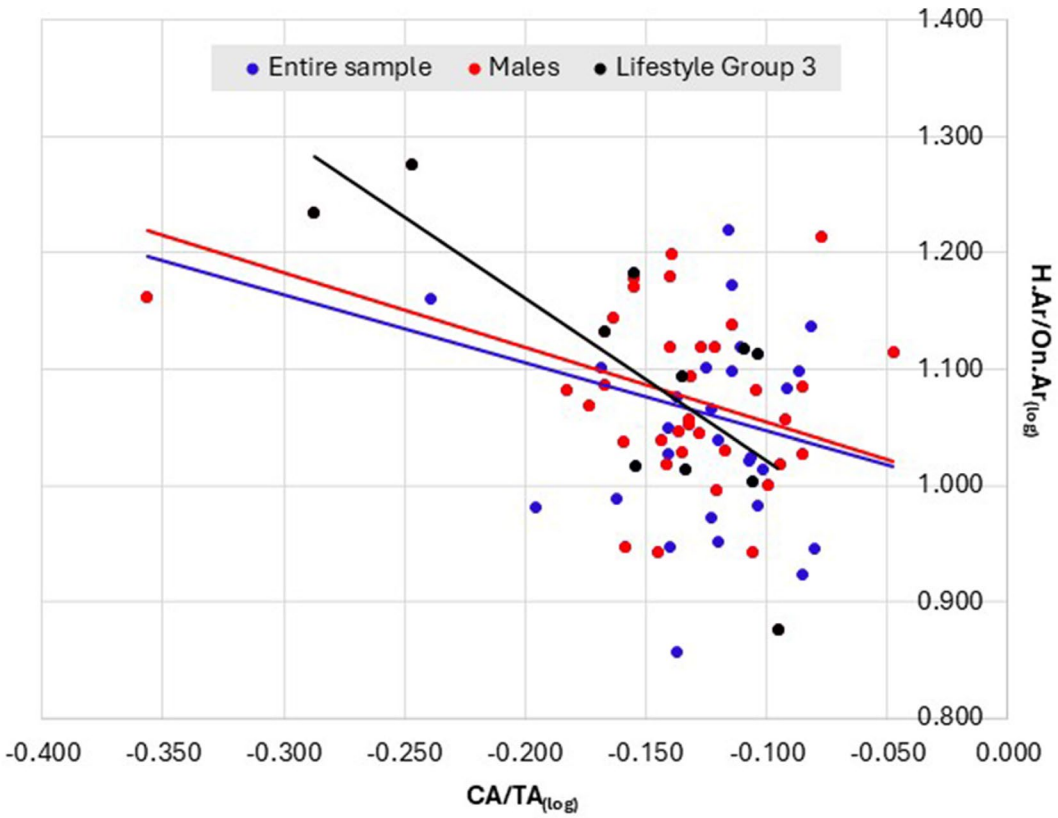

FIGURE 7 Regression graph for allometric relationships between log cortical/total area (CA/TA) and log Haversian canal to secondary osteon area (H.Ar/On. Ar) in the entire sample (blue markers and trendline, $n = 73$), males (red markers and trendline, $n = 39$) and one lifestyle group of sedentary but well-nourished individuals (black markers and trendline, $n = 11$). Note, outliers were retained as there was no biological or other reason to exclude them. Table 6 contains the reduced major axis regression statistics.

(Greendale et al., 1999). When developing our hypothesis, we proposed that if present, those allometries would be independent of sex because we assumed them to be a universal intra-specific constraint (Klingenberg, 2005). However, could our results point to other sex-related factors that possibly cloud a relationship of static allometry?

Other sex-related factors include larger body size, larger muscles, more mechanical stimulation on bone and thus more robust bones associated with differences in habitual activity in males compared to females (Riggs et al., 2004; Taaffe et al., 2003). Considering our I_{max}/I_{min} and CA/TA data, such differences are very minor and not statistically significant, with young and older males having slightly larger I_{max}/I_{min} (indicating larger midshafts with higher resistance to bending) than young and older females, yet CA/TA follows this pattern only in the young group. The older females in our sample appear to have higher values for CA/TA than older males. The impact of sexual dimorphism or sex-related physical activity on skeletal build thus only partly explains the allometric correlations in the males. A related factor, however, could be an interaction between physical activity and diet. The one other sub-group with a significant allometric relationship was in the lifestyle group of sedentary but well-nourished individuals. This suggests that their limited physical activity did not lead to any mechanically induced stimulation of bone remodelling and thus did not cloud the allometric relationship with their stochastic remodelling likely well sustained through good nutrition (Bonjour et al., 2009). This might explain why the other lifestyle groupings did not yield an allometry, as those groups either had mechanical stimulation (the active and well-nourished group) that could add extra bone density or were sedentary and poorly nourished which could have led to poor bone quality. The lifestyle that we termed 'ordinary' is likely a group of a combination of lifestyles, since it included reports that did not note specifically sedentary or active behaviours.

From a biomechanical perspective, our results do not correspond with findings from other studies using human cadaver long bones. For example, Goldman et al. (2014) in a study of 10 human (male and female) cadaver tibiae found a positive relationship between tibia robusticity and secondary osteon size such that robust bones had more secondary osteons and larger pores when compared to slender bones. Their study, however, did not test for allometry and focused more on biomechanical stimulation that is responsible for overall bone slenderness and robusticity, concluding that when remodelling is locally regulated, it is likely modulated by some form of bone size signal that suppresses remodelling in slender bones. If that is the case in all human long bones, then it could explain why we observed no allometry in the other lifestyle groups, particularly group 2 with active lifestyles, meaning that their histology represented a mechanical rather than anatomical signal. Our histology data did originate from sub-periosteal cortical bone regions which are known to generate additional bone in the face of activity induced modelling (in addition to remodelling) (Robling et al., 2006). Further, Tommasini et al. (2005) found in 17 male donors that bone mechanical properties varied with bone morphology suggesting that internal bone (micro)architecture is capable of compensating for macroscopic constraints. Similarly, Jepsen et al. (2011) using peripheral quantitative computed tomography (pQCT) scans of >600 tibiae in males and females reported a compensatory mechanism of bone cells that mediates remodelling in slender and robust bones without compromising microarchitecture. They proposed that it was the tensile or compressive stiffness modulus variation with bone size that mattered more than bone microarchitecture for mechanical competence. Finally, Epelboym et al. (2012), in the femoral necks from 49 female cadavers studied pQCT, micro-computed tomography, and ash-content analysis, found that bone loss patterns differed between slender and robust bones appearing that each had its own set of morphological traits.

Overall, two implications emerge from our findings in the context of prior published literature: thicker femoral midshaft could be determining less porous secondary osteons (thick-walled secondary osteons with relatively smaller Haversian canals), but this relationship is not straightforward in cases of morphological extremes, such as where a bone is very slender or robust. Given that there is very little variation in the CA/TA and I_{max}/I_{min} values in our study, the size of the midshaft is largely homogenous unlike in Goldman et al. (2014), Jepsen et al. (2011) and Epelboym et al. (2012). From the perspective of secondary osteon trade-offs (higher porosity favouring metabolic processes vs lower porosity favouring mechanical competence), our finding points to favouring increased mechanical robustness at the femoral midshaft when the growth between cortical wall and its secondary osteons is understood within broader anatomical constraints.

There are several limitations in our study. First, the imperfect categorisation of lifestyles based on the autopsy and next-of-kin questionnaires inherently relied on recall from secondary sources for each individual and their interpretation of what constitutes an active or sedentary lifestyle. For responses about older individuals, this interpretation by next-of-kin may have further implications, as they may consider an individual active across their lifespan when they had been less active in recent years due to age or changes in lifestyle. This is an important distinction when examining bone microstructure that reflects the last ~10 years of life and may be at odds with what was described in the survey data. As such, it is not possible to identify a point, or points, or periods of lifespan represented by the lifestyle information. Second, the sample size in our study varied between sub-groups also creating limitations for statistical analyses. Third, we do not have access to femoral length measurements, which could be used to calculate femur robusticity indices providing a further dimension on cortical wall proportions of the midshaft (Stock & Shaw, 2007). We have no mineralisation, microcrack or collagen fibre orientation data for these samples, but these could add another dimension from a biomechanical point of view. Lastly, any genetic underpinning to bone morphology and microstructure was not possible to measure in the sample and so the known skeletal variance associated with genetic variance remains unaccounted for. We recommend future research uses a range of bone visualisation techniques and quantifies allometric relationships in bones other than the femur to test whether and how macro–microscopic relationships are present throughout the human skeleton.

5 | CONCLUSIONS

In this study we examined femur midshaft cortical bone histology and cross-sectional geometry in a sample of 73 human individuals from Melbourne, Australia. We tested for static allometry between these two microscopic and macroscopic perspectives, by regressing secondary osteon area, the proportion of Haversian canal and secondary osteon area, and secondary osteon population density against the proportion of cortical-to-total area of the cross-section and the proportion of axes of the largest and smallest femur rigidity areas. We found negative allometry in cortical-to-total midshaft femur area and Haversian canal-to-secondary osteon area in the entire sample, in the males, and in a sub-group of individuals who likely led sedentary lifestyles but of good nourishment. Our data indicated that femoral midshafts with thicker cortical walls grew correspondingly less porous, thick-walled secondary osteons, which agrees with some prior research in humans and other mammals. Based on these results, we suggest that future bone remodelling and histology research of long bones takes into account macroscopic measures of bone size to account for any scaling effects on histological parameters. As our findings were not evident across all age, sex and lifestyle sub-groups, we also emphasise the complexity of human bone remodelling.

AUTHOR CONTRIBUTIONS

JJM: Concept/design, acquisition of data, data analysis/interpretation, drafting of the manuscript, critical revision and funding; LABW: Contributions to concept/design, interpretation and critical revision of the manuscript; KMC: Contributions to concept/design, interpretation and critical revision of the manuscript; RH: Contributions to concept/design, materials, acquisition of data, data analysis/interpretation and critical revision of the manuscript.

ACKNOWLEDGMENTS

We dedicate this paper to the late John Clement. We thank Ariane Maggio for technical advice. JJM thanks the University of Melbourne for facilitating access to next-of-kin and autopsy questionnaires in their care. This study was funded by the Australian Research Council (JJM: FT240100030; DE190100068, LABW: FT200100822). We thank two anonymous reviewers for their constructive feedback on the original version of our manuscript. Open access publishing facilitated by The University of Queensland, as part of the Wiley - The University of Queensland agreement via the Council of Australasian University Librarians

DATA AVAILABILITY STATEMENT

Raw data sharing, including autopsy and questionnaire content, is restricted under ethics protocol. Histology data for secondary osteon area and derived histology and cross-sectional geometry variables are available open access from figshare: http://doi.org/10.6084/m9.figshare.29083304.

ORCID

Justyna J. Miszkiewicz https://orcid.org/0000-0002-9769-2706
Laura A. B. Wilson https://orcid.org/0000-0002-3779-8277
Karen M. Cooke https://orcid.org/0000-0002-3022-6508

REFERENCES

Allen, M.R. & Burr, D.B. (2019) Bone growth, modeling, and remodeling. In: Burr, D.B. & Allen, M.R. (Eds.) *Basic and applied bone biology*. San Diego: Academic Press, pp. 85–100.

Basilia, P., Miszkiewicz, J.J., Nganvongpanit, K., Zaim, J., Rizal, Y., Aswan et al. (2023) Bone histology in a fossil elephant (*Elephas maximus*) from Pulau Bangka, Indonesia. *Historical Biology*, 35, 1356–1367. Available from: https://doi.org/10.1080/08912963.2022.2092850

Beresheim, A.C., Pfeiffer, S.K. & Alblas, A. (2018) The influence of body size and bone mass on cortical bone Histomorphometry in human ribs. *The Anatomical Record*, 301, 1788–1796. Available from: https://doi.org/10.1002/ar.23933

Bonjour, J.-P., Guéguen, L., Palacios, C., Shearer, M.J. & Weaver, C.M. (2009) Minerals and vitamins in bone health: the potential value of dietary enhancement. *British Journal of Nutrition*, 101, 1581–1596. Available from: https://doi.org/10.1017/S0007114509311721

Bousson, V., Meunier, A., Bergot, C., Vicaut, É., Rocha, M.A., Morais, M.H. et al. (2001) Distribution of Intracortical porosity in human Midfemoral cortex by age and gender. *Journal of Bone and Mineral Research*, 16, 1308–1317. Available from: https://doi.org/10.1359/jbmr.2001.16.7.1308

Britz, H.M., Thomas, C.D.L., Clement, J.G. & Cooper, D.M.L. (2009) The relation of femoral osteon geometry to age, sex, height and weight. *Bone*, 45, 77–83. Available from: https://doi.org/10.1016/j.bone.2009.03.654

Burr, D.B. (1992) Estimated intracortical bone turnover in the femur of growing macaques: implications for their use as models in skeletal pathology. *The Anatomical Record*, 232, 180–189. Available from: https://doi.org/10.1002/ar.1092320203

Chang, B. & Liu, X. (2022) Osteon: structure, turnover, and regeneration. *Tissue Engineering Part B: Reviews*, 28, 261–278. Available from: https://doi.org/10.1089/ten.teb.2020.0322

Chen, Y., Hu, X. & Liu, W. (2022) Modelling of bone fracture using the fundamental functional unit—osteon. *Theoretical and Applied Fracture Mechanics*, 118, 103216. Available from: https://doi.org/10.1016/j.tafmec.2021.103216

Cheverud, J.M. (1982) Relationships among ontogenetic, static, and evolutionary allometry. *American Journal of Physical Anthropology*, 59, 139–149. Available from: https://doi.org/10.1002/ajpa.1330590204

Clarke, V. & Braun, V. (2017) Thematic analysis. *The Journal of Positive Psychology*, 12, 297–298. Available from: https://doi.org/10.1080/17439760.2016.1262613

Cooke, K.M., Mahoney, P. & Miszkiewicz, J.J. (2022) Secondary osteon variants and remodeling in human bone. *The Anatomical Record*, 305, 1299–1315. Available from: https://doi.org/10.1002/ar.24646

Cowin, S.C. & Cardoso, L. (2015) Blood and interstitial flow in the hierarchical pore space architecture of bone tissue. *Journal of Biomechanics*, 48(5), 842–854. Available from: https://doi.org/10.1016/j.jbiomech.2014.12.013

Dominguez, V.M. & Agnew, A.M. (2016) Examination of factors potentially influencing osteon size in the human rib. *The Anatomical Record*, 299(3), 313–324. Available from: https://doi.org/10.1002/ar.23305

Doube, M. (2022) Closing cones create conical lamellae in secondary osteonal bone. *Royal Society Open Science*, 9, 220712. Available from: https://doi.org/10.1098/rsos.220712

Doube, M., Kłosowski, M.M., Arganda-Carreras, I., Cordelières, F.P., Dougherty, R.P., Jackson, J.S. et al. (2010) BoneJ: free and extensible bone image analysis in ImageJ. *Bone*, 47(6), 1076–1079. Available from: https://doi.org/10.1016/j.bone.2010.08.023

Epelboym, Y., Gendron, R.N., Mayer, J., Fusco, J., Nasser, P., Gross, G. et al. (2012) The interindividual variation in femoral neck width is associated with the acquisition of predictable sets of morphological and tissue-quality traits and differential bone loss patterns. *Journal*

of Bone and Mineral Research, 27, 1501–1510. Available from: https://doi.org/10.1002/jbmr.1614

Feik, S.A., Thomas, C.D.L., Bruns, R. & Clement, J.G. (2000) Regional variations in cortical modeling in the femoral mid-shaft: sex and age differences. *American Journal of Physical Anthropology*, 112, 191–205. Available from: https://doi.org/10.1002/(SICI)1096-8644(2000)112:2<191::AID-AJPA6>3.0.CO;2-3

Felder, A.A., Phillips, C., Cornish, H., Cooke, M., Hutchinson, J.R. & Doube, M. (2017) Secondary osteons scale allometrically in mammalian humerus and femur. *Royal Society Open Science*, 4, 170431. Available from: https://doi.org/10.1098/rsos.170431

Forriol, F. & Jedrzejczak, A. (2023) Bone structure and metabolism. In: Longo, U.G. & Denaro, V. (Eds.) *Textbook of musculoskeletal disorders*. Cham: Springer International Publishing, pp. 3–13. Available from: https://doi.org/10.1007/978-3-031-20987-1_1

Frost, H.M. (1987) Secondary osteon population densities: an algorithm for estimating the missing osteons. *American Journal of Physical Anthropology*, 30, 239–254. Available from: https://doi.org/10.1002/ajpa.1330300513

Gocha, T.P. & Agnew, A.M. (2016) Spatial variation in osteon population density at the human femoral midshaft: histomorphometric adaptations to habitual load environment. *Journal of Anatomy*, 228, 733–745. Available from: https://doi.org/10.1111/joa.12433

Goldman, H.M., Hampson, N.A., Guth, J.J., Lin, D. & Jepsen, K.J. (2014) Intracortical remodeling parameters are associated with measures of bone robustness. *The Anatomical Record*, 297, 1817–1828. Available from: https://doi.org/10.1002/ar.22962

Goodyear, S.R., Gibson, I.R., Skakle, J.M.S., Wells, R.P.K. & Aspden, R.M. (2009) A comparison of cortical and trabecular bone from C57 black 6 mice using Raman spectroscopy. *Bone*, 44, 899–907. Available from: https://doi.org/10.1016/j.bone.2009.01.008

Gosman, J.H., Hubbell, Z.R., Shaw, C.N. & Ryan, T.M. (2013) Development of cortical bone geometry in the human femoral and tibial diaphysis. *The Anatomical Record*, 296(5), 774–787. Available from: https://doi.org/10.1002/ar.22688

Greendale, G.A., Lee, N.P. & Arriola, E.R. (1999) The menopause. *The Lancet*, 353, 571–580. Available from: https://doi.org/10.1016/S0140-6736(98)05352-5

Grizzo, F.M.F., Alarcão, A.C.J., Dell'Agnolo, C.M., Pedroso, R.B., Santos, T.S., Vissoci, J.R.N. et al. (2020) How does women's bone health recover after lactation? A systematic review and meta-analysis. *Osteoporosis International*, 31, 413–427. Available from: https://doi.org/10.1007/s00198-019-05236-8

Heaney, R.P., Abrams, S., Dawson-Hughes, B., Looker, A., Looker, A., Marcus, R. et al. (2000) Peak bone mass. *Osteoporosis International*, 11, 985–1009. Available from: https://doi.org/10.1007/s001980070020

Hinkle, D.E., Wiersma, W., Jurs, S.G. & Cox, J.R. (2003) *Applied statistics for the behavioral sciences: applying statistical concepts workbook*, 5th edition. Boston: Houghton Mifflin.

Jepsen, K.J., Centi, A., Duarte, G.F., Galloway, K., Goldman, H., Hampson, N. et al. (2011) Biological constraints that limit compensation of a common skeletal trait variant lead to inequivalence of tibial function among healthy young adults. *Journal of Bone and Mineral Research*, 26, 2872–2885. Available from: https://doi.org/10.1002/jbmr.497

Jowsey, J. (1966) Studies of Haversian systems in man and some animals. *Journal of Anatomy*, 100, 857–864.

Kerley, E.R. (1965) The microscopic determination of age in human bone. *American Journal of Physical Anthropology*, 23, 149–163. Available from: https://doi.org/10.1002/ajpa.1330230215

Klingenberg, C.P. (2005) Developmental constraints, modules, and Evolvability. In: Hallgrímsson, B. & Hall, B.K. (Eds.) *Variation*. Burlington: Academic Press, pp. 219–247. Available from: https://doi.org/10.1016/B978-012088777-4/50013-2

Koh, N.Y.Y., Miszkiewicz, J.J., Fac, M.L., Wee, N.K.Y. & Sims, N.A. (2024) Preclinical rodent models for human bone disease, including a focus on cortical bone. *Endocrine Reviews*, 45, 493–520. Available from: https://doi.org/10.1210/endrev/bnae004

Matsuo, H., Tsurumoto, T., Maeda, J., Saiki, K., Okamoto, K., Ogami-Takamura, K. et al. (2019) Investigating interindividual variations in cortical bone quality: analysis of the morphotypes of secondary osteons and their population densities in the human femoral diaphysis. *Anatomical Science International*, 94, 75–85. Available from: https://doi.org/10.1007/s12565-018-0452-z

Mills, E.G., Yang, L., Nielsen, M.F., Kassem, M., Dhillo, W.S. & Comninos, A.N. (2021) The relationship between bone and reproductive hormones beyond estrogens and androgens. *Endocrine Reviews*, 42, 691–719. Available from: https://doi.org/10.1210/endrev/bnab015

Mishra, S. (2009) Biomechanical aspects of bone microstructure in vertebrates: potential approach to palaeontological investigations. *Journal of Biosciences*, 34, 799–809. Available from: https://doi.org/10.1007/s12038-009-0061-z

Mishra, S. & Knothe Tate, M. (2004) Allometric scaling relationships in microarchitecture of mammalian cortical bone. In: *50th annual meeting of the Orthopaedic Research Society*, San Francisco, p. 401.

Miszkiewicz, J.J., Athanassiou, A., Lyras, G.A. & van der Geer, A.A.E. (2023) Rib remodelling changes with body size in fossil hippopotamuses from Cyprus and Greece. *Journal of Mammalian Evolution*, 30, 1031–1046. Available from: https://doi.org/10.1007/s10914-023-09688-y

Miszkiewicz, J.J. & Mahoney, P. (2016) Ancient human bone microstructure in medieval England: comparisons between two socio-economic groups. *The Anatomical Record*, 299, 42–59. Available from: https://doi.org/10.1002/ar.23285

Miszkiewicz, J.J. & Mahoney, P. (2019) Histomorphometry and cortical robusticity of the adult human femur. *Journal of Bone and Mineral Metabolism*, 37, 90–104. Available from: https://doi.org/10.1007/s00774-017-0899-3

Miszkiewicz, J.J., Stewart, T.J., Naseri, R. & Sołtysiak, A. (2022) The lifestyles of bronze age Zagros highlanders at Deh Dumen, Iran: insights from midshaft femur cross-sectional geometry and histology. *Archaeometry*, 64, 1270–1287. Available from: https://doi.org/10.1111/arcm.12781

Miszkiewicz, J.J. & van der Geer, A.A.E. (2022) Inferring longevity from advanced rib remodelling in insular dwarf deer. *Biological Journal of the Linnean Society*, 136, 41–58. Available from: https://doi.org/10.1093/biolinnean/blac018

Paine, R.R. & Brenton, B.P. (2006) Dietary health does affect histological age assessment: an evaluation of the stout and paine (1992) age estimation equation using secondary from the rib. *Journal of Forensic Sciences*, 51, 489–492. Available from: https://doi.org/10.1111/j.1556-4029.2006.00118.x

Paine, R.R. & Godfrey, L.R. (1997) The scaling of skeletal microanatomy in non-human primates. *Journal of Zoology*, 241, 803–821. Available from: https://doi.org/10.1111/j.1469-7998.1997.tb05749.x

Pedersen, L.T., Miszkiewicz, J., Cheah, L.C., Willis, A. & Domett, K.M. (2024) Age-dependent change and intraskeletal variability in secondary osteons of elderly Australians. *Journal of Anatomy*, 244, 1078–1092. Available from: https://doi.org/10.1111/joa.14010

Pélabon, C., Firmat, C., Bolstad, G.H., Voje, K.L., Houle, D., Cassara, J. et al. (2014) Evolution of morphological allometry. *Annals of the New York Academy of Sciences*, 1320, 58–75. Available from: https://doi.org/10.1111/nyas.12470

Proia, P., Amato, A., Drid, P., Korovljev, D., Vasto, S. & Baldassano, S. (2021) The impact of diet and physical activity on bone health in children and adolescents. *Frontiers in Endocrinology*, 12, 704647. Available from: https://doi.org/10.3389/fendo.2021.704647

Riggs, B.L., Melton, L.J., III, Robb, R.A., Camp, J.J., Atkinson, E.J., Peterson, J.M. et al. (2004) Population-based study of age and sex differences in bone volumetric density, size, geometry, and structure at different skeletal sites. *Journal of Bone and Mineral Research*, 19, 1945–1954. Available from: https://doi.org/10.1359/jbmr.040916

Robling, A.G., Castillo, A.B. & Turner, C.H. (2006) Biomechanical and molecular regulation of bone remodeling. *Annual Review of Biomedical Engineering*, 8, 455–498. Available from: https://doi.org/10.1146/annurev.bioeng.8.061505.095721

Ruff, C.B. (2018) Quantifying skeletal robusticity. In: *Skeletal variation and adaptation in Europeans*. Hoboken, NJ: John Wiley & Sons, Ltd, pp. 39–47. Available from: https://doi.org/10.1002/9781118628430.ch3

Sahni, S. & Kiel, D.P. (2015) Smoking, alcohol, and bone health. In: Holick, M.F. & Nieves, J.W. (Eds.) *Nutrition and bone health*. New York, NY: Springer, pp. 489–504. Available from: https://doi.org/10.1007/978-1-4939-2001-3_30

Schindelin, J., Rueden, C.T., Hiner, M.C. & Eliceiri, K.W. (2015) The ImageJ ecosystem: an open platform for biomedical image analysis. *Molecular Reproduction and Development*, 82, 518–529. Available from: https://doi.org/10.1002/mrd.22489

Šešelj, M., Nahhas, R.W., Sherwood, R.J., Chumlea, W.C., Towne, B. & Duren, D.L. (2012) The influence of age at menarche on cross-sectional geometry of bone in young adulthood. *Bone*, 51, 38–45. Available from: https://doi.org/10.1016/j.bone.2012.03.030

Sheng, B., Li, X., Nussler, A.K. & Zhu, S. (2021) The relationship between healthy lifestyles and bone health: a narrative review. *Medicine*, 100, e24684. Available from: https://doi.org/10.1097/MD.0000000000024684

Skedros, J.G. (2024) Biomechanical foundations of histological analysis in limb bones: the crucial role of load-complexity categorization and collagen fiber orientation analysis when interpreting bone adaptation. In: *Bone histology: a biological anthropological perspective*, 2nd edition. Boca Raton: CRC Press, pp. 150–224.

Skedros, J.G., Knight, A.N., Clark, G.C., Crowder, C.M., Dominguez, V.M., Qiu, S. et al. (2013) Scaling of Haversian canal surface area to secondary osteon bone volume in ribs and limb bones. *American Journal of Physical Anthropology*, 151, 230–244. Available from: https://doi.org/10.1002/ajpa.22270

Skedros, J.G., Mason, M.W., Nelson, M.C. & Bloebaum, R.D. (1996) Evidence of structural and material adaptation to specific strain features in cortical bone. *The Anatomical Record*, 246, 47–63. Available from: https://doi.org/10.1002/(SICI)1097-0185(199609)246:1<47::AID-AR6>3.0.CO;2-C

Skedros, J.G., Mason, M.W. & Bloebaum, R.D. (1994) Differences in osteonal micromorphology between tensile and compressive cortices of a bending skeletal system: indications of potential strain-specific differences in bone microstructure. *The Anatomical Record*, 239, 405–413. Available from: https://doi.org/10.1002/ar.1092390407

Smith, R.J. (2009) Use and misuse of the reduced major axis for line-fitting. *American Journal of Physical Anthropology*, 140, 476–486. Available from: https://doi.org/10.1002/ajpa.21090

Stock, J.T. & Shaw, C.N. (2007) Which measures of diaphyseal robusticity are robust? A comparison of external methods of quantifying the strength of long bone diaphyses to cross-sectional geometric properties. *American Journal of Physical Anthropology*, 134, 412–423. Available from: https://doi.org/10.1002/ajpa.20686

Stout, S. & Crowder, C. (2011) Bone remodeling, histomorphology, and histomorphometry. In: Crowder, C. & Stout, S.D. (Eds.) *Bone histology: an anthropological perspective*. Boca Raton: CRC Press, pp. 1–21.

Stout, S.D. & Paine, R.R. (1994) Bone remodeling rates: a test of an algorithm for estimating missing osteons. *American Journal of Physical Anthropology*, 93, 123–129. Available from: https://doi.org/10.1002/ajpa.1330930109

Taaffe, D.R., Lang, T.F., Fuerst, T., Cauley, J.A., Nevitt, M.C. & Harris, T.B. (2003) Sex- and race-related differences in cross-sectional geometry and bone density of the femoral mid-shaft in older adults. *Annals of Human Biology*, 30, 329–346. Available from: https://doi.org/10.1080/0301446031000089588

Thomas, C.D.L., Feik, S.A. & Clement, J.G. (2005) Regional variation of intracortical porosity in the midshaft of the human femur: age and sex differences. *Journal of Anatomy*, 206(2), 115–125. Available from: https://doi.org/10.1111/j.1469-7580.2005.00384.x

Tommasini, S.M., Nasser, P., Schaffler, M.B. & Jepsen, K.J. (2005) Relationship between bone morphology and bone quality in male tibias: implications for stress fracture risk. *Journal of Bone and Mineral Research*, 20, 1372–1380. Available from: https://doi.org/10.1359/JBMR.050326

Ulrich, U., Miller, P.B., Eyre, D.R., Chesnut, C.H., Schlebusch, H. & Soules, M.R. (2003) Bone remodeling and bone mineral density during pregnancy. *Archives of Gynecology and Obstetrics*, 268, 309–316. Available from: https://doi.org/10.1007/s00404-002-0410-8

Ural, A. & Vashishth, D. (2006) Interactions between microstructural and geometrical adaptation in human cortical bone. *Journal of Orthopaedic Research*, 24, 1489–1498. Available from: https://doi.org/10.1002/jor.20159

Zedda, M. & Babosova, R. (2021) Does the osteon morphology depend on the body mass? A scaling study on macroscopic and histomorphometric differences between cow (*Bos taurus*) and sheep (*Ovis aries*). *Zoomorphology*, 140, 169–181. Available from: https://doi.org/10.1007/s00435-021-00516-6

SUPPORTING INFORMATION

Additional supporting information can be found online in the Supporting Information section at the end of this article.

How to cite this article: Miszkiewicz, J.J., Wilson, L.A.B., Cooke, K.M. & Hardiman, R. (2026) Scaling relationships between Haversian canal-to-secondary osteon and midshaft femur cortical-to-total area in a human autopsy sample. *Journal of Anatomy*, 00, 1–18. Available from: https://doi.org/10.1111/joa.70143